A MODEL FOR HEDGING LOAD AND PRICE RISK IN THE TEXAS ELECTRICITY MARKET

Michael Coulon (corresponding author)
Address: ORFE Department
Princeton University
Princeton NJ 08544, USA
Telephone: 609 258 5894
Fax: 609 258 3791
Email: mcoulon@princeton.edu

Warren B. Powell
Address: ORFE Department
Princeton University
Princeton NJ 08544, USA
Email: powell@princeton.edu

Ronnie Sircar
Address: ORFE Department
Princeton University
Princeton NJ 08544, USA
Email: sircar@princeton.edu

A MODEL FOR HEDGING LOAD AND PRICE RISK IN THE TEXAS ELECTRICITY MARKET

Abstract. Energy companies with commitments to meet customers' daily electricity demands face the problem of hedging load and price risk. We propose a joint model for load and price dynamics, which is motivated by the goal of facilitating optimal hedging decisions, while also intuitively capturing the key features of the electricity market. Driven by three stochastic factors including the load process, our power price model allows for the calculation of closed-form pricing formulas for forwards and some options, products often used for hedging purposes. Making use of these results, we illustrate in a simple example the hedging benefit of these instruments, while also evaluating the performance of the model when fitted to the Texas electricity market.

Keywords: electricity market; structural model; spikes; forward prices; spread options; hedging
JEL Classification Numbers: C60, C80, G12, G13, Q40

1. Introduction

In recent years, the use of financial products, such as futures and options, by retail suppliers to hedge electricity price and demand spikes has grown. The occurrence of spikes in electricity markets, as well as their relationship to loads (energy demands) which have strong seasonal components, requires non-standard financial models. On the other hand, having continuous-time stochastic models built around Brownian motion, as is typical for understanding options in financial markets, allows for convenient pricing formulas which can reduce the simulation burden on an optimization program for hedging risk.

The model we propose aims to capture the unique features and complex dependence structure of electricity price and load dynamics while retaining enough mathematical tractability to allow for such pricing results. In particular, we include as state variables the key factors which drive electricity prices, such as fuel price (natural gas in particular), load itself, and a proxy for capacity available. We express power spot price as a parametric function of underlying factors, including an additional 'regime' to describe the risk of extreme price spikes, which are most likely to occur when demand is relatively high, for example during times of unexpectedly high temperatures. We also model periodicity and seasonality in load and price at various time horizons to reflect hourly patterns, weekends, and also annual effects. Despite the rich dependence structure embedded in the model, convenient formulas for derivatives prices are available, facilitating the calibration to market data and the model's application to hedging problems.

We choose to analyze data from the US electricity market in Texas, often referred to as ERCOT (Electric Reliability Council of Texas), after the name of the ISO (Independent System Operator) which manages the Texas Interconnection power grid. Along with the Eastern and Western Interconnections, it is one of the three main electricity grids in the US and serves over 20 million customers. As in many electricity markets around the world, deregulation in Texas occurred approximately ten years ago. Since then, the highly volatile and quite dramatic behaviour of prices has drawn much attention to the challenges of electricity price modeling. Given the growth of intermittent wind energy in Texas and the state's susceptibility to heat waves and other extreme weather, features such as price spikes are particularly important for the ERCOT market. A strong

Date: August 2012.

reminder of this was provided by the heat wave of early August 2011, when the total load hit a record level of 68.4 GWh, and day-ahead prices for peak afternoon hours reached their cap of $3000 per MWh on several consecutive days. Such extreme events may be even more dramatic in the future, following a recent decision by ERCOT to increase the cap to $4500 effective August 2012 and to increase it to as high as $9000 by 2015.

Much of the literature on quantitative models for electricity prices has focused on extending traditional finance approaches to account for these spikes, for example through jump processes. Such approaches typically begin by specifying a stochastic process directly for the electricity spot price, possibly incorporating several unobservable factors, seasonal functions and sometimes multiple regimes (typically lasting just a few hours, so one should not interpret the terminology 'regime' to mean a lasting paradigm shift). An early single-factor model by [8] uses a jump diffusion process, while [16] separates the jumps from the diffusion in a two-factor version to account for very rapid recovery from price spikes. In [14], the authors instead propose a threshold level above which jumps become negative to recover from spikes, while several authors (cf, [24, 12]) have instead suggested regime-switching models to handle sudden spikes and rapid recoveries. In [4], a general framework based on sums of Levy processes is advocated, which can allow for some convenient results for forward prices, while in [23] the authors apply multivariate Levy semistationary processes to the EEX market in Europe. Another alternative is the use of heavy-tailed distributions such as the Cauchy distribution, as presented in [18] and applied to two US markets, PJM and ERCOT.

While the above works differ extensively in both their motivations and mathematical details, they all share the characteristic of taking spot electricity prices as the starting point for a stochastic model, thus placing them in the category of 'reduced-form' models. While such approaches may be successful for capturing price spikes and overall price distributions, they rarely capture the complicated dependence structure between price, load and other factors, which is equally vital for hedging purposes in practice. Hence, we instead favor the category often known as 'structural' models, as reviewed for example in the recent survey paper of [6]. In such a model, power price is written as a function of several underlying supply and demand factors, and its dynamics are therefore not specified directly through an SDE (stochastic differential equation), but produced indirectly as a result of the dynamics chosen for the factors. Early work by Barlow [3] treated demand as the only driving factor, before various authors extended this branch of the literature to include factors such as fuel prices [20, 7], capacity changes [5, 10], or both [11, 2].

A benefit of the structural approach is that it makes use of readily available information on fundamentals such as market load and in some cases supply side information like generation costs. However, for mathematical tractability, it stops short of a full description of all the details of the price setting mechanism such as operational and transmission constraints, instead simply approximating the shape of the electricity stack. Nonetheless, it reflects key features of load and price dynamics, such as the observation that times of high load are more likely to produce price spikes, for example when the highest cost and least efficient units are forced to run to satisfy demand. This close relationship between load and price is important for energy companies to understand when hedging the risk of either physical asset ownership or their obligations to serve retail customers at predetermined price levels. However, the relationship between price and load is blurred by effects such as outages, transmission problems and other constraints or shocks which can sometimes produce price spikes even at periods of low or average demand. Such complications of the electricity grid create a challenge for structural models that rely on a clear and consistent relationship between price and load. Adding additional unobservable factors such as jump processes is a common reduced-form solution to such obstacles, but less in the spirit of the structural approach.

We therefore propose a model which builds on the structural approaches mentioned above, but also incorporates some ideas from the reduced-form literature in order to obtain a better fit to the ERCOT market. In particular, we extend the typical stack-based methodology (e.g., as in [20, 11, 1]) to include a 'spike regime', in which the price-to-load relationship adjusts to reflect such times of extreme market conditions. Within each regime, the power price is lognormal, but we show that the mixing of these lognormals can produce the heavy-tailed price densities observed in the market. The probability of being in the spike regime is also assumed to be load-dependent, yet we retain the important advantage of closed-form solutions for forward and option prices, exploiting convenient properties of multivariate Gaussian distributions. Section 2 introduces the model, while Section 3 presents the results for forwards, as well as parameter estimation and calibration. In Section 4, we present the related closed-form option pricing results and then in Section 5 study an application of the model to hedging an obligation to serve customer load. Finally we conclude in Section 6.

2. Model & Motivation

The electricity price model consists of several separate pieces, corresponding to each of the underlying stochastic factors followed by their link with spot power price. In this section, we address each of these in turn, and introduce the parameters and notation.

2.1. **Load.** The primary short-term driver for electricity prices is load, which is the starting point of our analysis. Later we will incorporate the longer-term effects of fuel prices, specifically through natural gas prices. Figure 1a shows the striking seasonal variation in daily average load. In fact

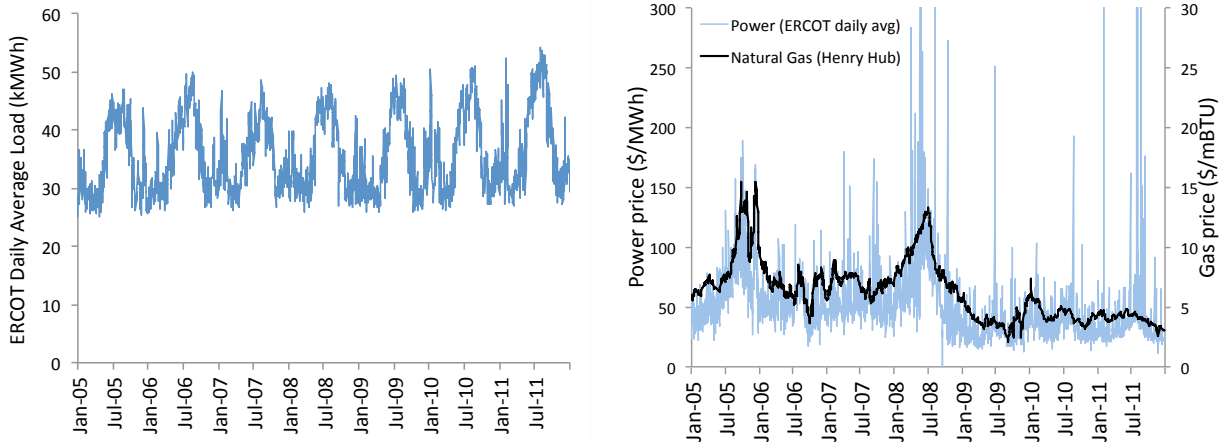

(A) Historical daily average ERCOT loads

(B) Historical daily average electricity and gas prices

FIGURE 1. *ERCOT load and electricity prices over 2005-11. Note that we choose to plot daily average power prices only for the range $0 to $300. However, during the period 2005-11, there were nine days with averages above $300 (including five in August 2011), and two days in Sept 2008 with averages just below zero (due to several hourly values below -$200).*

as Figure 2 shows, the seasonal pattern varies significantly hour to hour throughout the day. For example, hour 8 has both a summer and a winter peak, while hour 16 only has a summer peak and a much greater peak to trough ratio. There are also periodicities caused by weekends when businesses are closed.

We first de-seasonalize the ERCOT load L_t:

$$L_t = S(t) + \bar{L}_t,$$

where the seasonal component (estimated using hourly data) is given by

$$S(t) = a_1(h) + a_2(h)\cos(2\pi t + a_3(h)) + a_4(h)\cos(4\pi t + a_5(h)) + a_6(h)t + a_7(h)\mathbf{1}_{we}.$$

Here h is the hour, and $\mathbf{1}_{we}$ is an indicator variable for weekends; a_2 to a_5 are the seasonal components, a_6 picks up the upward trend visible in Figure 1a, and a_7 captures the drop in demand on weekends. Figure 2 shows the fitted seasonal components for hours 8 and 16.

Then we fit the residual load $\bar{L}_t$ to an Ornstein-Uhlenbeck (OU) model:

$$d\bar{L}_t = -\kappa_L \bar{L}_t\, dt + \eta_L\, dW_t^{(L)}.$$

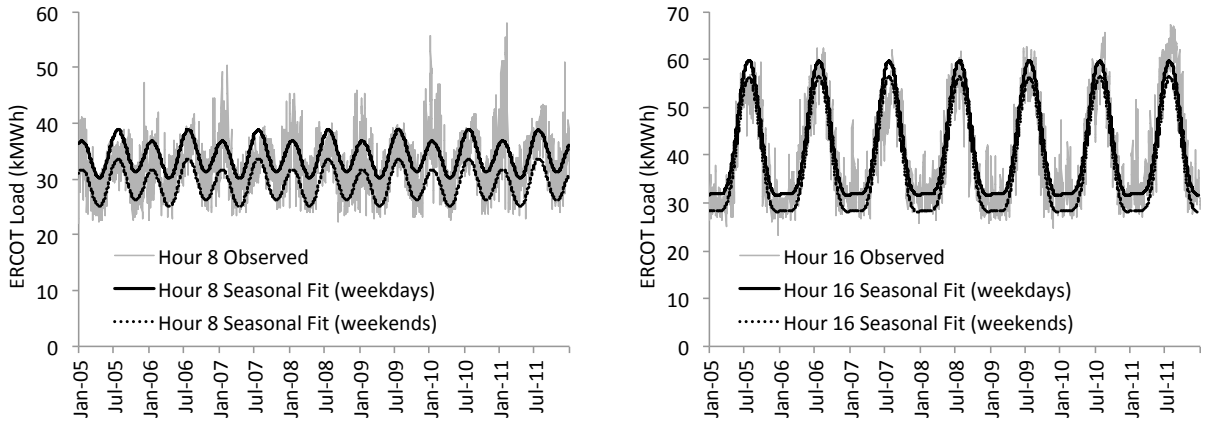

(A) Hour 8 (B) Hour 16

FIGURE 2. *ERCOT load over 2005-11 for chosen hours, along with fitted seasonality functions.*

2.2. **Structural Electricity Model.** From Figure 1b, we observe that electricity prices exhibit high volatility and numerous spikes, and they seem to fluctuate around a level driven by natural gas prices. We use the well-known one-factor Schwartz model [21] in which the gas price G_t is the exponential of an OU process:

$$d\log G_t = \kappa_G(m_G - \log G_t)\, dt + \eta_G\, dW_t^{(G)},$$

where $W^{(L)}$ and $W^{(G)}$ are independent.

We also introduce an additional factor X which proxies for the effect of capacity outages and grid congestion, and is given by

$$X_t = S_X(t) + \bar{X}_t,$$

with seasonal component treated similarly to that of load:

$$S_X(t) = b_1(h) + b_2(h)\cos(2\pi t + b_3(h)) + b_4(h)\cos(4\pi t + b_5(h)).$$

The process $\bar{X}_t$ follows

$$d\bar{X}_t = -\kappa_X \bar{X}_t\, dt + \eta_X\, dW_t^{(X)},$$

where the Brownian motions $W^{(X)}$ and $W^{(L)}$ are correlated with parameter ν. Note that $\bar{L}$ and $\bar{X}$ are assumed to be mean-zero OU processes, since their mean levels are incorporated into $S(t)$ and $S_X(t)$ respectively.

While we pose our model in continuous time to take advantage of the convenient properties of Brownian motion, we note that in reality spot power is observed at discrete times, only once per hour (in most markets). See, for instance, the discussion in [4, Section 1.5]. Therefore any spike is only observed at an hourly frequency, and so we use the following regime-switching model for P_t which is driven by a sequence of independent random variables m_k defined for times $t_k \in \mathcal{T} = \{t_1, t_2, \ldots\}$, the set containing the start of every hour. At each t_k, the value of $m_k \in \{1, 2\}$ is determined by an independent coin flip whose probabilities depend on the current load $\bar{L}_{t_k}$:

$$m_k = \begin{cases} 1 & \text{with probability } 1 - p_s \Phi\left(\frac{\bar{L}_{t_k} - \mu_s}{\sigma_s}\right) \\ 2 & \text{with probability } p_s \Phi\left(\frac{\bar{L}_{t_k} - \mu_s}{\sigma_s}\right), \end{cases} \tag{1}$$

where p_s, μ_s and σ_s are positive constants and $\Phi(\cdot)$ is the standard Gaussian cumulative distribution function (cdf). Then, for each time t,

$$P_t = G_t \exp(\alpha_{m_k} + \beta_{m_k} L_t + \gamma_{m_k} X_t) \quad \text{for } t_k \leq t < t_{k+1}, k \in \mathbb{N}. \tag{2}$$

Hence, m_k determines each hour whether we are in the 'normal' regime (with parameters $\alpha_1, \beta_1, \gamma_1$) or the 'spike' regime (with parameters $\alpha_2, \beta_2, \gamma_2$). Note that the parameter γ_1 is a redundant parameter in the model fitting since X_t is an unobserved variable. Thus γ_1 could be set equal to 1 if desired, but we choose to keep it for notational symmetry, and hence more convenient formulas later. The parameter p_s represents the maximum spike probability (ie, as $\bar{L}_t \to \infty$), while μ_s and σ_s control the precise dependence on load. A sensible choice for the parameters μ_s and σ_s is the mean and standard deviation of the stationary distribution of deseasonalized load $\bar{L}_t$, such that the probability of a spike is then linear in the quantile of load:

$$\mu_s = 0, \qquad \sigma_s = \frac{\eta_L}{\sqrt{2\kappa_L}} \tag{3}$$

This model has three stochastic factors, gas G_t, load L_t and the additional factor X_t, as well as a regime switching mechanism to capture spikes. We comment on each of these:

- The gas multiplies a function which can be interpreted as approximating the range of generator heat rates in the market. This multiplicative structure has been proposed by other authors (cf. [20, 13, 7]) and reflects the fact that fuel costs are typically the dominant driver of the production cost curve, which in turn determines bid levels.
- The empirical relationship between price and load is typically convex and often modelled with an exponential function (c.f.[22, 10, 19]), as less efficient generators are used only at peak demand times, producing significantly higher prices. Often driven primarily by temperature, demand is well-known to be mean-reverting (around seasonal levels) and often chosen to be Gaussian as proposed here.
- The additional factor X_t is not strictly equal to market capacity, but represents all additional factors including most notably changes in capacity available and short-term outages or congestion-related events. In this way, we capture the additional volatility present in power prices which cannot be explained by load and gas price fluctuations alone.
- Finally, an important feature of the model is its second regime, which occurs with some 'spike probability', and allows us to reproduce the extremely heavy-tailed nature of the price distributions. Although both regimes have the same exponential form, the choice of $\alpha_2, \beta_2, \gamma_2$ allows for a steeper and potentially more volatile price to load relationship. In addition, as spikes are observed to increase in likelihood as load increases (but do also occur

at off-peak times), we allow the spike probability to depend on $\bar{L}_t$, and in particular to be linear in the quantile of the deseasonalized load distribution.

Notice that the resulting model for spot power prices is in fact a mixture of lognormal distributions, due to the choice of Gaussian processes for X_t, L_t and $\log G_t$. This convenient form will have benefits for the pricing of forwards and options, as we shall discuss later.

We note that various straightforward extensions to the set-up are possible. For example, we might add a third regime if we wish to include negative spikes (and negative prices), as is discussed further in [6]. The regime probabilities could also be allowed to be *piecewise* linear in load quantile, for example for markets in which spikes are only observed to occur for demand above some threshold level. Furthermore, in order to obtain longer duration spikes, the transitions between regimes could be driven by a Markov chain in which the previous hour's state affects the spike probability this hour. However, given the important load-dependence built into these probabilities, this extension would come at the cost of less convenient forward and option pricing results, with little benefit if we care more about the frequency of spikes than their exact timing or duration. Finally, while the current value of load provides some information about future spike probability, we might also incorporate additional forward-looking information about supply or demand (e.g., weather forecasts or outage schedules) into the regime probabilities, along the lines of [9]. However, for our current purposes, the simpler framework suffices.

2.3. **Empirical Evidence.** Empirical evidence from ERCOT provides justification for the form of the model proposed in (2) above. Firstly, as power prices in ERCOT are most often set by natural gas generators at the margin, the co-movement of gas and electricity prices over long time horizons is striking, as observed earlier in Figure 1b. This appears consistent with the multiplicative relationship proposed above, and further evidence is provided by Figure 3a which plots monthly average power prices against gas prices for the period 2005-11. As gas is the most slowly moving factor in the model (see parameter estimates later), taking monthly averages highlights this relationship more than others. The points in the scatter plot are fairly well fit by a straight line through the origin (with slope approximately 8, corresponding intuitively to the heat rate in MWh/mmBTU of the typical marginal unit), although exceptional months can occur, most notably the previously mentioned case of August 2011, responsible for the outlier in the upper left corner.

Next, Figure 3b illustrates the relationship between price and load in ERCOT via a scatter plot for all hours in the year 2011. By plotting only one year of data here, the relationship is clearer since gas prices moved relatively slowly during 2011. In addition, plotting log prices allows us to include the huge spikes (eg, up to the price cap of \$3000) while still illustrating clearly the strong relationship in the typical price region (between about \$20 and \$60). This relationship appears close to linear (as suggested in the model) for the vast majority of data points, although it is worth noting that on this log plot a significant lower tail of prices near zero is visible even after removing all prices below \$1. However, our focus in this model is not on these off-peak price drops but instead on the dramatic positive spikes. We observe that the majority of these spikes, as well as the largest spikes, tend to occur at times of very high demand, but that somewhat smaller spikes do occur at times of lower to medium demand. Figure 3c illustrates this same point by using a rough definition of a spike as a price three times the average monthly value in a given time period. The plot shows that the probability of a spike does indeed appear to increase roughly linearly (apart from the last data point) in the quantile of demand, as suggested by the model in (2).

It is important to understand that any one of the relationships between P_t and a single underlying factor will of course be weakened by the volatility of the other factors driving prices. For example, in Figure 3d, we repeat the scatter plot of Figure 3b, but with 2008 data added to the 2011 data (and

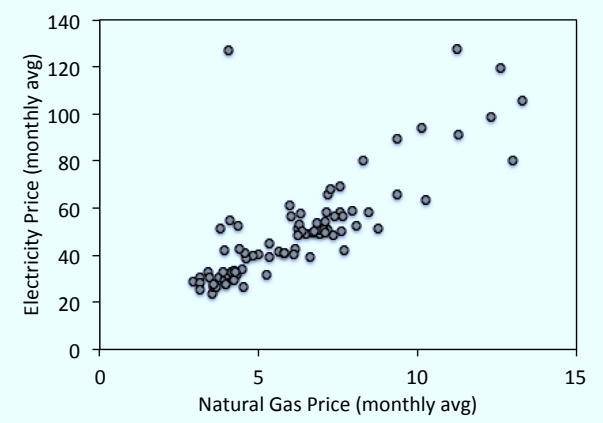

(A) Monthly average gas vs power

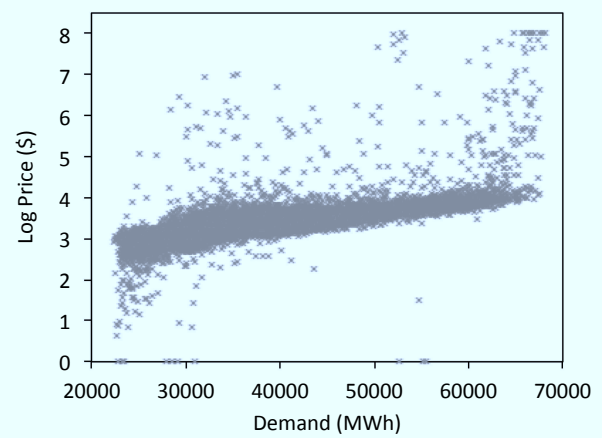

(B) Hourly price vs load for 2011

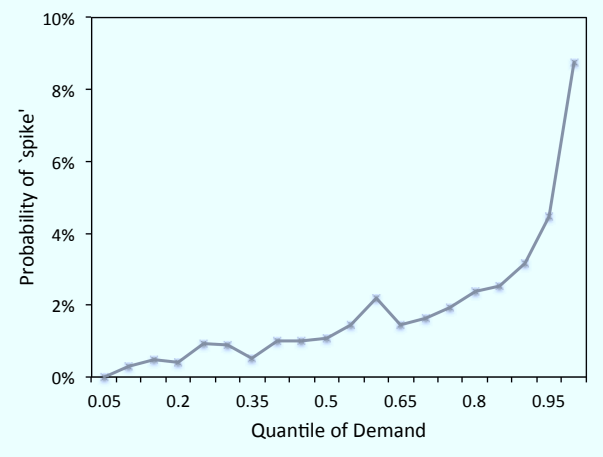

(C) Probability of spike vs load

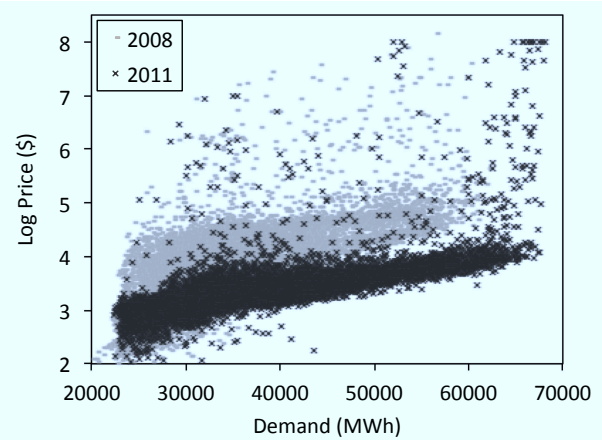

(D) Hourly price vs load for 2008 and 2011

FIGURE 3. Relationship between power price and gas price (top left), between power price and load (right column), and between spike probability and load (bottom left).

the price axis shifted slightly). Recall from Figure 1b that 2008 was a time of very high gas prices, and more generally record price levels throughout commodity markets. As a result, the entire cloud of 2008 points in the price-load scatter plot is shifted significantly upwards relative to the 2011 points. For each of the years, the linear relationship between log price and load is reasonably strong, but if combined together would be much weaker, causing difficulties for a structural model based *only* on load. This evidence thus highlights the importance of including gas prices in the model, both in order to better reproduce movements observed in historical data, and to capture this additional risk in future electricity price distributions. In Figure 4, we now plot the price ratio P_t/G_t against load L_t, thus avoiding the issue discussed above. Although we do not see the highest spikes in this plot, we do observe that the model's two exponential functions (one for each regime) can provide a reasonable fit to the data. We shall refer back to this plot when describing parameter estimation in the next section.

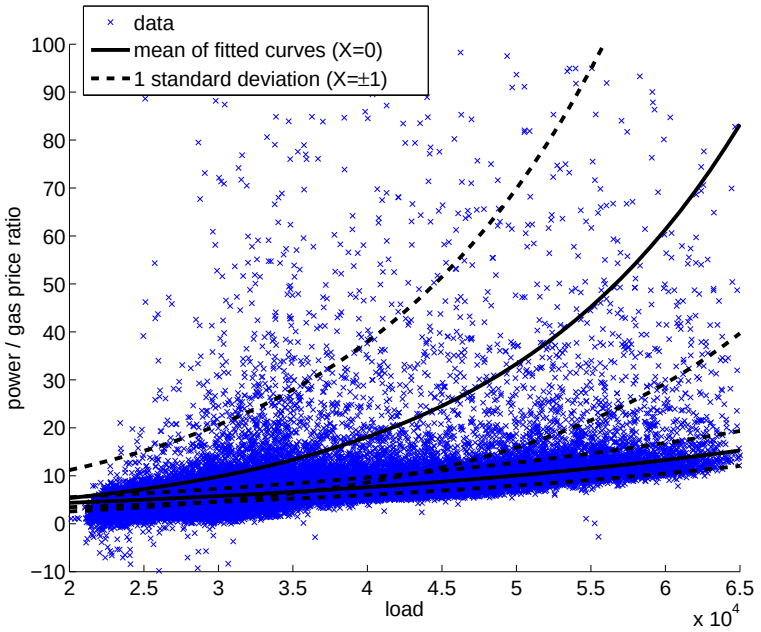

FIGURE 4. Fitting result - solid lines illustrate exponential price-load relationship when $X = 0$ (at the mean), while dotted lines represent one standard deviation bands ($X = \pm 1$). The y-axis has been truncated for illustration purposes: min and max values are -38 and 450 respectively.

3. Parameter Estimation & Forward Curve Calibration

Calibrating a model to market data is often a multi-step procedure, as will be the case here. We begin with historical data for electricity spot prices, gas prices and load, constructing estimation procedures for both the parameters driving the factor dynamics and those determining the shape of the electricity stack (the link between electricity price and its drivers). Next, we turn to electricity forward contracts, deriving explicit formulae for prices which can then be used to calibrate the model to observed forward quotes. It is important that a spot price model correctly price all available forward contracts in the market before being used to price other contracts or to tackle other problems.

3.1. **Parameter Estimation from History.** All model parameters are estimated using seven years of data (covering 2005-2011) for day-ahead ERCOT price and load, as well as Henry Hub spot gas prices. Maximum likelihood estimation (MLE) is used throughout, and the estimation procedure is divided into the following steps:

- We jointly estimate all parameters which appear in (2) given observed values of load and gas price,[1] and under the assumption that X_t is a standard Gaussian random variable at every t. This assumption is reasonable since we expect X to be a very fast mean-reverting process, reflecting short-term noise. Parameters γ_1 and γ_2 provide the appropriate scaling

[1]As we choose not to include a regime which allows for negative prices (or prices very near 0), we first remove all hourly data points for which $P_t/G_t \leq 0.1$ (only 132 out of over 61,000). In order to improve the fit in the regions we are interested in, we also iteratively exclude downward spikes of more than three standard deviations from the mean of the normal regime, while acknowledging that improvements would be needed to more accurately capture the price distribution near zero.

α_1	β_1	γ_1	α_2	β_2	γ_2	p_s
0.915	2.79e-05	0.237	0.453	6.11e-05	0.741	0.129

TABLE 1. Parameters relating to the power price function

Load		Natural Gas			Capacity / Noise		
κ_L	η_L	κ_G	m_G	η_G	κ_X	η_X	ν
92.59	53932	1.069	1.664	0.611	1517	66.07	-0.113

TABLE 2. Parameters relating to the stochastic processes for G_t, $\bar{L}_t$ and $\bar{X}_t$

for this process. The likelihood function $\mathcal{L}(\alpha_1, \beta_1, \gamma_1, \alpha_2, \beta_2, \gamma_2, p_s)$ that we maximize is

$$\mathcal{L} = \prod_t \left\{ p_s \Phi\left(\frac{\bar{L}_t - \mu_s}{\sigma_s}\right) \frac{1}{\gamma_2\sqrt{2\pi}} \exp\left(-\left(\frac{\log(P_t/G_t) - \alpha_2 - \beta_2 L_t}{\gamma_2}\right)^2\right) + \left(1 - p_s \Phi\left(\frac{\bar{L}_t - \mu_s}{\sigma_s}\right)\right) \frac{1}{\gamma_1\sqrt{2\pi}} \exp\left(-\left(\frac{\log(P_t/G_t) - \alpha_1 - \beta_1 L_t}{\gamma_1}\right)^2\right)\right\}. \tag{4}$$

- Next, given these parameters for the power price function (see Table 1), we use historical day-ahead electricity price data to back out the historical time series for X_t implied by the model, thus treating this factor as an unobserved residual process from the model.
- For both L and X, we find seasonality parameters by minimizing the sum of squared differences between historical values and the functions $S(t)$ and $S_X(t)$ respectively.[2]
- The OU process parameters for $\bar{L}_t$ and $\bar{X}_t$ are estimated by standard maximum likelihood estimation using the time series of hourly residuals after deseasonalization. This procedure is done jointly for $\bar{L}_t$ and $\bar{X}_t$ in order to accurately estimate their correlation. Finally, for natural gas, we repeat the same MLE procedure using (the logarithm of) Henry Hub spot prices, but observed at a daily level instead of hourly.

Note that for L and X, we allow the seasonality parameters to vary from hour to hour, but apply the OU fit to the single hourly time series of residuals since there is only one random factor driving each of these processes in the model. Table 2 shows the results of fitting the OU processes for all three factors. It is important to observe that the three factors move on very different time scales, with gas very slowly mean-reverting over months ($\kappa_G = 1.07$), load mean reverting over several days ($\kappa_L = 92.6$) and X_t mean reverting on an intra-day time scale ($\kappa_X = 1517$). In Table 1, we observe that $\beta_2 > \beta_1$, implying that in the spike regime the exponential relationship between price and load is significantly steeper, as expected in order to produce extreme spikes. In addition, since $\gamma_2 > \gamma_1$, the spike regime is also more volatile than the normal price regime, as is reflected in the scatter plot of Figure 3b. Note that $p_s = 0.129$ implies that we visit the spike regime approximately 6.5% of the time on average ($p_s/2$), since the probability at each t varies between 0 and 12.9% as $\bar{L}_t$ changes. Finally, the seasonal parameters for both $S(t)$ and $S_X(t)$ are listed in Table 3 and vary significantly from hour to hour, as was illustrated earlier in Figure 2.

Figure 4 shows the results of fitting the power price function, by plotting the ratio P_t/G_t against L_t for all hours in the dataset and then superimposing the fitted exponential curves. Since the price axis has been truncated from above, we can now see clearly the strong link between price and load in the 'normal regime', which is well captured by the function $\exp(\alpha_1 + \beta_1 L_t)$, represented by

[2]When implementing these functions, we use the convention that t equals the calendar time in years, such that for example the dataset begins on Jan 1st, 2005, when $t = 2005$.

Hour	Parameters for L_t							Parameters for X_t				
	a_1	a_2	a_3	a_4	a_5	a_6	a_7	b_1	b_2	b_3	b_4	b_5
1	30502	5881	2.989	-4019	3.023	0.00140	-1	0.092	0.044	2.984	0.322	2.621
2	29090	5015	2.957	-3905	3.011	0.00196	60	-0.196	0.119	4.086	0.274	3.025
3	28267	4270	2.934	-3833	3.003	0.00214	180	-0.419	0.081	6.062	0.208	3.111
4	27884	3681	2.911	-3794	3.023	0.00209	391	-0.553	0.244	6.545	0.130	3.408
5	28145	3128	2.883	-3816	3.006	0.00229	872	-0.464	0.425	6.482	0.113	3.223
6	29796	2438	2.796	-3896	3.011	0.00257	2174	-0.162	0.538	6.482	0.189	3.220
7	32880	1496	2.616	-3609	2.928	0.00286	4498	-0.376	0.578	6.512	0.258	3.467
8	34331	1145	2.526	-3521	2.959	0.00337	5160	-0.146	0.736	6.332	0.248	3.537
9	34823	2275	2.892	-3877	3.044	0.00673	3974	-0.155	0.477	6.376	0.217	2.957
10	35929	4097	2.968	-3951	3.063	0.00643	3229	0.080	0.392	6.288	0.185	2.807
11	37231	6247	2.995	-4161	3.014	0.00528	2993	0.212	0.326	6.141	0.151	2.985
12	38383	8337	2.998	-4244	2.962	0.00574	2911	0.135	0.316	6.163	0.166	2.813
13	39276	10125	2.998	-4466	2.926	0.00532	2891	0.124	0.123	5.570	0.253	3.145
14	40324	11730	3.000	-4488	2.883	0.00550	3195	0.180	0.085	4.418	0.356	3.242
15	41143	13073	2.998	-4367	2.854	0.00570	3389	0.204	0.205	3.459	0.455	3.202
16	41696	13943	3.008	-4193	2.842	0.00578	3471	0.193	0.328	3.406	0.557	3.250
17	42001	14182	3.011	-4105	2.854	0.00593	3469	0.250	0.282	3.374	0.585	3.136
18	42091	13447	2.997	-4162	2.970	0.00627	3165	0.253	0.122	6.491	0.454	2.742
19	41940	11490	2.964	-4823	3.085	0.00633	2804	0.300	0.669	6.295	0.221	2.074
20	41091	9845	2.961	-4675	3.013	0.00826	2515	0.156	0.710	6.332	0.179	3.058
21	40425	9189	2.978	-4114	2.953	0.00940	2377	0.104	0.501	5.925	0.365	3.429
22	39048	8785	3.029	-4234	3.016	0.00989	2055	-0.230	0.338	5.736	0.168	3.268
23	36200	7844	3.045	-4177	3.055	0.01103	1436	0.363	0.367	5.710	0.245	3.124
24	33053	6820	3.028	-4083	3.064	0.01543	901	0.025	0.170	5.673	0.331	2.836

TABLE 3. Parameters for load and capacity seasonality (ie, for functions $S(t)$ and $S_X(t)$)

the lower solid line. The upper solid line shows the function $\exp(\alpha_2 + \beta_2 L_t)$ for the 'spike regime' while the dotted lines around each solid line plot $\exp(\alpha_1 + \beta_1 L_t \pm \gamma_1)$ and $\exp(\alpha_2 + \beta_2 L_t \pm \gamma_2)$, indicating one standard deviation movements in X_t.

Note that since we do not constrain any parameters in the optimization, the 'spike' value may well turn out to be lower than the 'normal' value in some cases, especially for low load and large negative X_t, since $\gamma_2 > \gamma_1$. For example, at the far left of Figure 4, the $X_t = -1$ dotted line for spikes is almost \$1 below that of the normal regime. As a result, the value for $p_s = 12.9\%$ is larger than we might expect for maximum spike probability, particularly given Figure 3c. While on average $p_s/2 = 6.5\%$ of simulated points will be 'spikes', some of these will be very low values which do not appear as visible spikes in a time series, but instead mix with the 'normal' points. While this may be disadvantageous from the perspective of intuition, the fitting of a mixture of two lognormals inevitably requires some overlap, and our priority is an appropriate overall distribution. Finally, at first glance it may appear that there is a wider variation in prices for moderate L_t than for high L_t, but this is deceptive given the high density of points in the middle region, as well as the many spikes beyond the top of the plot.[3] Indeed, the standard deviation of $\log(P_t/G_t)$ given L_t is quite stable for different L_t ranges, lending support to the model.

[3]In fact, $L_t \in [30000, 40000]$ for nearly 50% of the data points, with about one quarter on either side of this range. Calling these three bins 'low', 'medium', and 'high' demand cases, we count that the proportion of points above the highest dotted line of Figure 4 is 0.58%, 0.90%, and 1.27% respectively for each bin, increasing slightly as we might expect given our load-dependent spike probabilities. If instead we count the proportion above the spike regime mean, we get 5.39%, 3.60% and 3.08% respectively. The decrease here can be explained by the visible overlap between regimes for lower L_t, whereby the normal regime can also produce high enough values to count.

3.2. **Power Forward Prices.** Forward and futures contracts are of utmost importance in electricity markets as they are often traded in much higher volumes than the spot and are crucial for the hedging needs of both producers and consumers of electricity. They come in many variations in different markets, including characteristics such as physical versus financial settlement and peak versus offpeak versus baseload delivery. In all cases, power forwards (or futures since we use the terms interchangeably here) have 'delivery periods' for which the electricity is bought or sold in advance. Therefore, instead of a single maturity T, the delivery is typically spread (uniformly) over a month (or season or year) long period, which can be represented instead by an interval $[T_1, T_2]$. In the case of physical delivery, a December 2012 baseload contract for example specifies delivery of (say) 1MW of power during every hour in the month of December 2012.

Since forward contracts have no upfront payment, standard no-arbitrage arguments imply that the forward price $F(t, [T_1, T_2])$ at time $t < T_1 < T_2$ is given by

$$F(t, [T_1, T_2]) = \frac{1}{(T_2 - T_1)/\Delta t} \sum_{T \in [T_1, T_2]} \mathbb{E}_t^{\mathbb{Q}}[P_T],$$

where Δt is the length of timestep in the delivery period (ie, one hour) and $\mathbb{E}_t^{\mathbb{Q}}$ denotes the time t conditional expectation under the risk-neutral pricing measure $\mathbb{Q}$. We assume for now that the risk-neutral measure is known in the market, or can be uniquely determined from available traded instruments.

As L and X are not themselves traded, we require an assumption about their market prices of risk in order to write down their dynamics under $\mathbb{Q}$. Either a constant or deterministic market price of risk implies that the processes remain OU processes under $\mathbb{Q}$, with unchanged speed of mean reversion and volatility. In other words, only their mean levels change, and so under $\mathbb{Q}$,

$$\begin{aligned} d\bar{L}_t &= \kappa_L(m_L - \bar{L}_t)\, dt + \eta_L\, dW_t^{(L)}, \\ d\bar{X}_t &= \kappa_X(m_X(t) - \bar{X}_t)\, dt + \eta_X\, dW_t^{(X)}, \end{aligned} \tag{5}$$

where $W^{(X)}$ and $W^{(L)}$ are now $\mathbb{Q}$-Brownian motions correlated with parameter ν. We also assume that under $\mathbb{Q}$, the power price P_t is still given by (2), as it was under the physical measure $\mathbb{P}$.

Notice that we assume a constant mean level m_L for the load process, but instead a time-dependent mean level $m_X(t)$ for the additional factor X. This choice allows for a convenient approach to calibrating the model to observed market forward quotes, a natural first priority of any spot price model before tackling other derivative pricing or hedging problems. Analogously to the Hull-White approach to yield curve calibration (see [17]), an appropriately chosen time-dependent mean-reversion level allows the model correctly price forwards of all maturities. Furthermore, this calibration procedure is also a way of identifying a risk-neutral measure $\mathbb{Q}$ which is consistent with no arbitrage in the market. In particular, since we typically observe only one forward contract for each calendar month (ignoring the issue of peak and off-peak forwards), we suggest choosing $m_X(t)$ to be a piecewise constant function with one jump per month. Each constant can be found successively using the forward price for the next available maturity. The availability of the closed-form expression for forward prices in coming pages greatly facilitates and speeds up this procedure.

For simplicity, we now consider the forward price $F^p(t, T)$ for a hypothetical contract with delivery at a single maturity T. Since $F^p(t, T) = \mathbb{E}_t^{\mathbb{Q}}[P_T]$, the expression above is simply an average over forward contracts for single hours. In order to calculate $F^p(t, T)$ in our model, we first require the conditional distribution of X_T given L_T under the risk-neutral measure $\mathbb{Q}$. Note that given $\bar{X}_t$

and $\bar{L}_t$, $\bar{X}_T$ and $\bar{L}_T$ are bivariate Gaussian with parameters $\{\mu_X, \sigma_X, \mu_L, \sigma_L, \rho\}$, where

$$\begin{pmatrix} \bar{X}_T \\ \bar{L}_T \end{pmatrix} \sim N\left(\begin{pmatrix} \mu_X \\ \mu_L \end{pmatrix}, \begin{pmatrix} \sigma_X^2 & \rho\sigma_X\sigma_L \\ \rho\sigma_X\sigma_L & \sigma_L^2 \end{pmatrix} \right)$$

and means and variances are all time dependent (although we will typically suppress (t,T) to ease notation):

$$\mu_X(t,T) = \bar{X}_t \mathrm{e}^{-\kappa_X(T-t)} + \kappa_X \int_t^T m_X(u) e^{-\kappa_X(T-u)} du, \tag{6}$$

$$\sigma_X^2(t,T) = \frac{\eta_X^2}{2\kappa_X}\left(1 - \mathrm{e}^{-2\kappa_X(T-t)}\right), \tag{7}$$

$$\mu_L(t,T) = \bar{L}_t \mathrm{e}^{-\kappa_L(T-t)} + m_L\left(1 - \mathrm{e}^{-\kappa_L(T-t)}\right), \tag{8}$$

$$\sigma_L^2(t,T) = \frac{\eta_L^2}{2\kappa_L}\left(1 - \mathrm{e}^{-2\kappa_L(T-t)}\right), \tag{9}$$

$$\rho(t,T) = \left(\frac{1}{\sigma_X\sigma_L}\right)\frac{\nu\eta_X\eta_L}{\kappa_X+\kappa_L}\left(1 - \mathrm{e}^{-(\kappa_X+\kappa_L)(T-t)}\right). \tag{10}$$

Hence the conditional distribution of X_T given L_T is

$$X_T|L_T \sim N\left(S_X(T) + \mu_X + \frac{\sigma_X}{\sigma_L}\rho(\bar{L}_T - \mu_L), (1-\rho^2)\sigma_X^2\right).$$

Note also that the forward price of gas is denoted $F^g(t,T)$ and satisfies $F^g(t,T) = \mathbb{E}_t^{\mathbb{Q}}[G_T]$. Then the forward price of power is found as follows:

$$\begin{aligned} F^p(t,T) &= \mathbb{E}_t^{\mathbb{Q}}\left[\mathbb{E}_t^{\mathbb{Q}}[P_T|L_T]\right] \\ &= \mathbb{E}_t^{\mathbb{Q}}\left[G_T \exp\left(\alpha_1 + \beta_1 L_T\right)\mathbb{E}_t^{\mathbb{Q}}[\exp(\gamma_1 X_T)|L_T]\left(1 - p_s\Phi\left(\frac{\bar{L}_T - \mu_s}{\sigma_s}\right)\right)\right. \\ &\qquad \left. + G_T \exp\left(\alpha_2 + \beta_2 L_T\right)\mathbb{E}_t^{\mathbb{Q}}[\exp(\gamma_2 X_T)|L_T]\, p_s\Phi\left(\frac{\bar{L}_T - \mu_s}{\sigma_s}\right)\right] \\ &= F^g(t,T)\mathbb{E}_t^{\mathbb{Q}}\left[\exp(k_1 + l_1\bar{L}_T)\left(1 - p_s\Phi\left(\frac{\bar{L}_T - \mu_s}{\sigma_s}\right)\right) + \exp(k_2 + l_2\bar{L}_T)\, p_s\Phi\left(\frac{\bar{L}_T - \mu_s}{\sigma_s}\right)\right] \end{aligned}$$

where k_i and l_i for $i \in \{1,2\}$ are functions of time given by

$$k_i(t,T) = \alpha_i + \beta_i S(T) + \gamma_i\left(S_X(T) + \mu_X - \frac{\sigma_X}{\sigma_L}\rho\mu_L + \frac{1}{2}\gamma_i(1-\rho^2)\sigma_X^2\right), \tag{11}$$

$$l_i(t,T) = \beta_i + \gamma_i\rho\frac{\sigma_X}{\sigma_L}. \tag{12}$$

This expectation is then computed using the following relationship (for constants a,b,c):

$$\int_{-\infty}^{\infty} \mathrm{e}^{cx}\Phi\left(a + bx\right)\frac{1}{\sqrt{2\pi}}\mathrm{e}^{-\frac{1}{2}x^2}dx = \mathrm{e}^{\frac{1}{2}c^2}\Phi\left(\frac{a+bc}{\sqrt{b^2+1}}\right). \tag{13}$$

This is a special case of a formula in [7, 6] which conveniently rewrites the integral of the product of an exponential, a univariate Gaussian density and Gaussian cdf as a simple bivariate Gaussian cdf (which collapses again to a univariate cdf when integrating over $(-\infty,\infty)$ as above). In this

case, we obtain the following closed-form expression:

$$(14)\quad F^p(t,T) = F^g(t,T)\left[\exp\left(k_1+l_1\mu_L+\frac{1}{2}l_1^2\sigma_L^2\right)\left(1-p_s\Phi\left(\frac{\mu_L-\mu_s+l_1\sigma_L^2}{\sqrt{\sigma_L^2+\sigma_s^2}}\right)\right)\right.$$
$$\left.+\exp\left(k_2+l_2\mu_L+\frac{1}{2}l_2^2\sigma_L^2\right)p_s\Phi\left(\frac{\mu_L-\mu_s+l_2\sigma_L^2}{\sqrt{\sigma_L^2+\sigma_s^2}}\right)\right].$$

Given (3), for large enough time to maturity $(T-t)$, when $\bar{L}_T$ is well approximated by its stationary distribution (ie, for more than a week or so since $\kappa_L = 92.6$), (14) can be written as

$$F^p(t,T) = F^g(t,T)\left[\exp\left(k_1+l_1m_L+\frac{l_1^2\eta_L^2}{4\kappa_L}\right)\left(1-p_s\Phi\left(\frac{l_1\eta_L}{\sqrt{4\kappa_L}}\right)\right)\right.$$
$$\left.+\exp\left(k_2+l_2m_L+\frac{l_2^2\eta_L^2}{4\kappa_L}\right)p_s\Phi\left(\frac{l_2\eta_L}{\sqrt{4\kappa_L}}\right)\right].$$

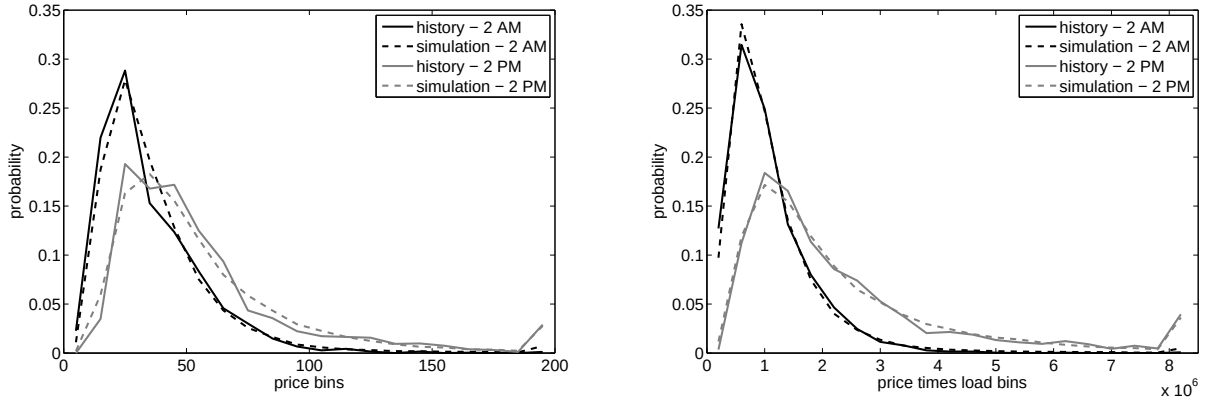

(A) Price (B) Price times Load

FIGURE 5. Histograms for P_t (left) and $P_t \times L_t$ (right): model simulation vs. historical data

3.3. **Model Performance.** The histograms in Figure 5 provide some evidence of the model's ability to capture hourly price distributions accurately. These plots were generated by simulating 100 paths of seven years of price and load dynamics, while always using the historical gas prices from the seven years of data (2005-2011). As natural gas price is a slowly moving factor in the model, its dynamics over a single seven-year period can vary widely. Therefore, in order to isolate the load-to-price relationship and obtain a more meaningful comparison with historical data, we have chosen to fix the path of gas price movements to match with history.

For illustration purposes, we plot one representative peak hour (2pm) and one representative off-peak hour (2am), which can be observed to differ significantly. Nonetheless, despite being driven by the same sources of randomness, simulated trajectories for 2am and 2pm capture these differences quite well through the seasonality functions $S(t)$ and $S_X(t)$. In addition to simply analyzing price, the right plot shows histograms for price times load, which will be particularly important later in our hedging example. The figures indicate that the correlation structure between price and load is well reproduced by the model.

4. Option Pricing Formulas

As noted above, the availability of an explicit formula for $F^p(t,T)$, the forward price of power, is a significant advantage of the model proposed in Section 2. We now show that in certain cases, option prices are also available in closed-form. We consider call options on both electricity alone and on the spread between electricity and gas, and note that analogous results are available for put options. Finally, we make use of these derivative pricing results in a simple example of hedging, in which a load-serving utility firm wishes to minimize the variance of his revenues by hedging with forwards or options.

4.1. Options on Spot Power.

We begin with a simple call option with strike K and maturity T on the electricity spot price P_T. We assume a constant interest rate r. The option price V_t^p at time t can be calculated as follows, first conditioning on L_T as was the case for forward prices:

$$\begin{aligned}
V_t^p &= \mathrm{e}^{-r(T-t)}\mathbb{E}_t^{\mathbb{Q}}\left[(P_T-K)^+\right] \\
&= \mathrm{e}^{-r(T-t)}\mathbb{E}_t^{\mathbb{Q}}\left[\mathbb{E}_t^{\mathbb{Q}}[(P_T-K)^+|L_T]\right] \\
&= \mathrm{e}^{-r(T-t)}\mathbb{E}_t^{\mathbb{Q}}\left[\mathbb{E}_t^{\mathbb{Q}}\left[\left(G_T\exp\left(\alpha_1+\beta_1 L_T+\gamma_1 X_T\right)-K\right)^+|L_T\right]\left(1-p_s\Phi\left(\frac{\bar{L}_T-\mu_s}{\sigma_s}\right)\right)\right. \\
&\qquad \left. + \mathbb{E}_t^{\mathbb{Q}}\left[\left(G_T\exp\left(\alpha_1+\beta_1 L_T+\gamma_1 X_T\right)-K\right)^+|L_T\right]p_s\Phi\left(\frac{\bar{L}_T-\mu_s}{\sigma_s}\right)\right]
\end{aligned}$$

Each of the inner expectations corresponds to pricing a call option on a lognormal asset, and thus can be found using the following variation of Black's formula: If $Y\sim N\left(\mu_Y,\sigma_Y^2\right)$, then

$$\mathbb{E}\left[\left(\mathrm{e}^Y-K\right)^+\right]=\mathrm{e}^{\mu_Y+\frac{1}{2}\sigma_Y^2}\Phi\left(\frac{\mu_Y+\sigma_Y^2-\log K}{\sigma_Y}\right)-K\Phi\left(\frac{\mu_Y-\log K}{\sigma_Y}\right)$$

Hence, the resulting integrand contains the product of Black's formula and the regime probability functions, both of which include univariate Gaussian cdfs of linear functions of $\bar{L}_T$, a Gaussian random variable. Hence, for the outer expectation we require integrating over a bivariate Gaussian cdf (with correlation zero in this case), and make use of the following result, which is analogous to (13) but in higher dimensions and is a special case of a formula in [6] involving the trivariate Gaussian cdf:

$$\int_{-\infty}^{\infty}e^{cx}\Phi_2\left(a_1+b_1x,a_2+b_2x;\rho\right)\frac{\mathrm{e}^{-\frac{1}{2}x^2}}{\sqrt{2\pi}}dx=\mathrm{e}^{\frac{1}{2}c^2}\Phi_2\left(\frac{a_1+b_1c}{\sqrt{b_1^2+1}},\frac{a_2+b_2c}{\sqrt{b_2^2+1}};\frac{b_1b_2+\rho}{\sqrt{(b_1^2+1)(b_2^2+1)}}\right) \tag{15}$$

where $a_1,a_2,b_1,b_2,c,\lambda$ are constants and $\Phi_2(\cdot,\cdot;\rho)$ is the standard bivariate Gaussian cumulative distribution function with correlation ρ.

After a few lines of algebra we eventually obtain

$$\begin{aligned}
V_t^p &= \mathrm{e}^{-r(T-t)}\left\{F^g(t,T)\exp\left(k_1+l_1\mu_L+\frac{1}{2}l_1^2\sigma_L^2\right)\Phi\left(d_1^+\right)-K\Phi\left(d_1^-\right)\right. \\
&+ \left. p_s\sum_{i=1}^{2}(-1)^i\left[F^g(t,T)\exp\left(k_i+l_i\mu_L+\frac{1}{2}l_i^2\sigma_L^2\right)\Phi_2\left(d_i^+,g_i^+;\lambda_i\right)-K\Phi_2\left(d_i^-,g_i^-;\lambda_i\right)\right]\right\} \qquad (16)
\end{aligned}$$

where

$$d_i^+ = \frac{k_i + l_i\mu_L + \frac{1}{2}l_i^2\sigma_L^2 + \log(F^g(t,T)/K) + \frac{1}{2}\varsigma_i^2}{\sqrt{\varsigma_i^2 + l_i^2\sigma_L^2}}, \qquad d_i^- = d_i^+ - \frac{\varsigma_i^2 + l_i^2\sigma_L^2}{\sqrt{\varsigma_i^2 + l_i^2\sigma_L^2}},$$

$$g_i^+ = \frac{\mu_L - \mu_s + l_i\sigma_L^2}{\sqrt{\sigma_s^2 + \sigma_L^2}}, \qquad g_i^- = g_i^+ - \frac{l_i\sigma_L^2}{\sqrt{\sigma_s^2 + \sigma_L^2}},$$

$$\lambda_i = \frac{l_i\sigma_L^2}{\sqrt{(\varsigma_i^2 + l_i^2\sigma_L^2)(\sigma_s^2 + \sigma_L^2)}}, \qquad \varsigma_i^2 = \frac{\eta_G^2}{2\kappa_G}\left(1 - \mathrm{e}^{-2\kappa_G(T-t)}\right) + \gamma_i^2(1-\rho^2)\sigma_X^2.$$

As the bivariate normal cdf is easy to implement using a built in function in most mathematical programming software (just like the univariate cdf), the option prices given by (16) very fast to compute, even though the formulas look a little complicated. This is of great benefit for example if we consider a portfolio of options on many different individual hours during a month-long or year-long period.

4.2. **Spread Options on Spot Power and Gas.** Now, consider instead a spread (or exchange) option on power and gas, with payoff $(P_T - hG_T)^+$, where h is a constant. Note that this payoff is sometimes used to approximate the revenue from owning a gas-fired power plant at time T with heat rate h and negligible non-fuel operating costs. See [7] for an example of power plant valuation based on this idea. In the current model, the calculation of the price $V_t^{p,g}$ of such an option proceeds very similarly to that shown above, and is in fact slightly simpler, since gas price G_T is independent and can be immediately factored out of the payoff function:

$$\begin{aligned} V_t^{p,g} &= \mathrm{e}^{-r(T-t)}\mathbb{E}_t^{\mathbb{Q}}\left[\mathbb{E}_t^{\mathbb{Q}}[(P_T - hG_T)^+|L_T]\right] \\ &= \mathrm{e}^{-r(T-t)}\mathbb{E}_t^{\mathbb{Q}}\left[G_T\mathbb{E}_t^{\mathbb{Q}}\left[\exp\left(\alpha_1 + \beta_1 L_T + \gamma_1 X_T\right) - h)^+ |L_T\right]\left(1 - p_s\Phi\left(\frac{\bar{L}_T - \mu_s}{\sigma_s}\right)\right)\right. \\ &\qquad \left. + G_T\mathbb{E}_t^{\mathbb{Q}}\left[\exp\left(\alpha_1 + \beta_1 L_T + \gamma_1 X_T\right) - h)^+ |L_T\right] p_s\Phi\left(\frac{\bar{L}_T - \mu_s}{\sigma_s}\right)\right]. \end{aligned}$$

Eventually we obtain

$$\begin{aligned} V_t^{p,g} &= \mathrm{e}^{-r(T-t)}F^g(t,T)\left\{\exp\left(k_1 + l_1\mu_L + \frac{1}{2}l_1^2\sigma_L^2\right)\Phi\left(\tilde{d}_1^+\right) - h\Phi\left(\tilde{d}_1^-\right)\right. \\ &\qquad \left. + p_s\sum_{i=1}^{2}(-1)^i\left[\exp\left(k_i + l_i\mu_L + \frac{1}{2}l_i^2\sigma_L^2\right)\Phi_2\big(\tilde{d}_i^+, \tilde{g}_i^+; \tilde{\lambda}_i\big) - h\Phi_2\big(\tilde{d}_i^-, \tilde{g}_i^-; \tilde{\lambda}_i\big)\right]\right\}, \end{aligned} \tag{17}$$

where

$$\tilde{d}_i^+ = \frac{k_i + l_i\mu_L + \frac{1}{2}l_i^2\sigma_L^2 - \log(h) + \frac{1}{2}\tilde{\varsigma}_i^2}{\sqrt{\tilde{\varsigma}_i^2 + l_i^2\sigma_L^2}}, \qquad \tilde{d}_i^- = \tilde{d}_i^+ - \frac{\tilde{\varsigma}_i^2 + l_i^2\sigma_L^2}{\sqrt{\tilde{\varsigma}_i^2 + l_i^2\sigma_L^2}},$$

$$\tilde{g}_i^+ = \frac{\mu_L - \mu_s + l_i\sigma_L^2}{\sqrt{\sigma_s^2 + \sigma_L^2}}, \qquad \tilde{g}_i^- = \tilde{g}_i^+ - \frac{l_i\sigma_L^2}{\sqrt{\sigma_s^2 + \sigma_L^2}},$$

$$\tilde{\lambda}_i = \frac{l_i\sigma_L^2}{\sqrt{(\tilde{\varsigma}_i^2 + l_i^2\sigma_L^2)(\sigma_s^2 + \sigma_L^2)}}, \qquad \tilde{\varsigma}_i^2 = \gamma_i^2(1-\rho^2)\sigma_X^2.$$

4.3. **Options on Forwards.** The majority of options traded in commodity markets (and especially on exchanges) reference forward prices as their underlying instead of spot prices. For example, one may want to price a call option with payoff $(F^p(T,T_f)-K)^+$ at T, or a spread option with payoff $(F^p(T,T_f)-hF^g(T,T_f))^+$, where the forwards have maturity T_f greater than the option maturity T. In practice a modification may often be required to this payoff due to the forward's delivery period, especially for options on calendar-month forwards. In this paper we ignore this complication, and concentrate instead on the simpler payoff structure, for which some closed-form expressions are feasible. Note that this category includes for example an option which allows the buyer to decide one day in advance of delivery whether to exercise or not (so $T_f - T = 1/365$).

An important observation when valuing options on forwards in our structural model is that the time scales of the dynamics of our factors vary widely between G_t (slowly mean-reverting over many months), L_t (fairly rapidly mean-reverting over several days) and X_t (extremely rapidly mean-reverting at an intra-day level). This is important for options on forwards, because the time $(T_f - T)$ between forward and option maturity dictates which distributions at time T will be important. For example, if $T_f - T$ is large enough that X_{T_f} conditional on time T information is already well-approximated by its stationary distribution, then the forward price $F^p(T,T_f)$ can be assumed independent of X_T, greatly simplifying calculations. Even though most exchange-traded options mature only a few business days before the beginning of the delivery period of the underlying forward contract, given our parameter estimate of $\kappa_X = 1517$, this is already long enough to make the above assumption and help to obtain some closed-form results.

In the case of options on electricity forwards, no closed-form expression is available, but pricing by simulation is straightforward and fast thanks to our expression for forwards in (14). On the other hand, for options on spreads between power and gas forwards, $F^g(T,T_f)$ can be pulled out of both the payoff function and the expectation, paving the way for a rather complicated formula for the option price. The result is in the spirit of Geske's closed-form formula for compound equity options [15], since it requires first calculating a value of load $\bar{L}_T^\star$ above which the option will be exercised. $\bar{L}_T^\star$ then appears inside a bivariate Gaussian cdf in the result, as presented in Appendix A.

5. Revenue Hedging

Despite the growth of interest in recent years from financial institutions, a large proportion of the trading in electricity forwards and options is carried out by producers and consumers, who hedge against both upwards and downwards price swings. In particular, we consider here the case of a retail power utility company, which is classified as a consumer, since it must buy power from the wholesale market in order to satisfy retail customer needs. Although the real consumers are individuals and businesses, these end-users are typically subject to a fixed (or slowly-varying) price per MWh, and hence the power company cannot simply pass on the risk of spot price movements to its customers. Instead, it faces the choice of waiting and buying the required amount of electricity each hour from the spot market, or hedging its obligations in advance through the purchase of forwards, options or some combination of the two. In some cases, utility companies also own generation assets which act as an alternative hedge for their obligations.

In this section, we shall consider a highly simplified version of this hedging decision, in which we are only concerned about delivery over a single day in the future, and we make a single hedging decision today. In other words, this is a *static* hedge, so we do not consider dynamically re-hedging through time as maturity approaches. Furthermore, we assume that the firm's load is perfectly correlated with the total ERCOT market load L_t, implying that the firm delivers to some fixed fraction of the market, say $w \in [0,1]$. (In one case study, we have found correlations of around 90%

between firm load and market load, with $w \approx 0.5\%$.) Setting $\tau = 1/365$ and p^{fixed} to be the price it charges its customers per MWh, the firm's revenue R_T over the one-day period $[T, T+\tau]$ in the future is given by

$$R_T = \sum_{j=1}^{24} wL_{T_j} \left(p^{fixed} - P_{T_j} \right), \quad \text{where } T_j = T + \frac{j}{24}\tau.$$

We allow trading in the following contracts in order to hedge the firm's risk:

- Forward contracts with delivery on a particular hour j, with price $F^p(t, T_j)$
- Call options on these forwards, with payoff at $T_j - \tau$ of $\tilde{V}^p_{T_j-\tau} = (F^p(T_j - \tau, T_j) - K(j))^+$
- Spark spread options on forwards, with payoff $\tilde{V}^{p,g}_{T_j-\tau} = (F^p(T_j - \tau, T_j) - hF^g(T_j - \tau, T_j))^+$
- Call options on the hourly spot power price, with payoff $V^p_{T_j} = \left(P_{T_j} - K(j)\right)^+$
- Spark spread options on spot energy prices, with payoff $V^{p,g}_{T_j} = \left(P_{T_j} - hG_{T_j}\right)^+$,

where h and $K(j)$ are the heat rates and strikes specified in the option contracts. We allow the hourly strikes to vary due to the large price variation through the day, and in the base case consider only at-the-money (ATM) options for all hours. In the base case, we also set t to be January 1st, 2013, and maturity $T = t + 1$ to be one year later, as well as fixing constants $r = 2\%, p^{fixed} = 50, w = 1$ and choosing current values $\bar{X}_t = \bar{L}_t = 0$ and $\log(G_t) = m_G$.

Note that we do not consider forwards with delivery periods here, but instead forwards on individual hours, with prices given explicitly by (14) in our model (and similarly for options on single hour spot prices, by (16) and (17)). As a result the spread options on forwards that we consider have prices also given in closed-form in (18) in the appendix. We comment that while exchange traded forward contracts do not reference specific hours, it is possible to trade such hourly forward contracts over the counter (OTC) for example through custom-made so-called 'shape' products which tailor to firms' expected intra-day demand profile. For options on forwards, it is possible to create and trade all sorts of different products by varying maturities and delivery periods, but for simplicity here we choose only options which have maturity one day before the delivery hour of the forward contract. In other words, the buyer must decide at the beginning of one day whether to buy power at strike $K(j)$ for each hour $j \in \{1, \ldots, 24\}$ of the following day.

As our example proposes a static hedge, we are not attempting to eliminate all risk. Instead, we aim to assess the degree to which each of the power price derivatives listed above can reduce the risk in the distribution of revenue R_T, which depends on load times price. Recall that since price is itself a function of load in this model, derivatives on price are implicitly also derivatives on load itself. As a measure of risk reduction, we take the common objective of variance minimization. The variance of the firm's profits at T can be written as

$$\text{Var}\left(R_T - \sum_{n=1}^{N} \theta_n U_T^{(n)} \right)$$

where the $\theta_1, \ldots, \theta_N$ represent the quantities purchased of N available hedging products with payoffs $U_T^{(1)}, \ldots, U_T^{(N)}$. For most of our analysis, we choose $N = 1$ to compare products one by one. The effectiveness of each hedge is determined by the covariance of R_T and $U_T^{(n)}$.

In addition, for simplicity we assume that there is no risk premium priced into forwards or options: $m_L = m_X = 0$ in (5) (and the risk-neutral measure $\mathbb{Q}$ coincides with the physical measure $\mathbb{P}$). As a consequence, the mean of our profit distribution is essentially unaffected by the number of forwards and options that we purchase. Therefore, the prices $U_t^{(1)}, \ldots, U_t^{(N)}$ of the products do

not appear in our objective function given above. While this is of course unrealistic, it allows us to focus solely on the variance aspect of the hedging problem, instead of requiring a more involved mean-variance analysis which would yield different conclusions depending on the risk premia of the different products traded in the market.

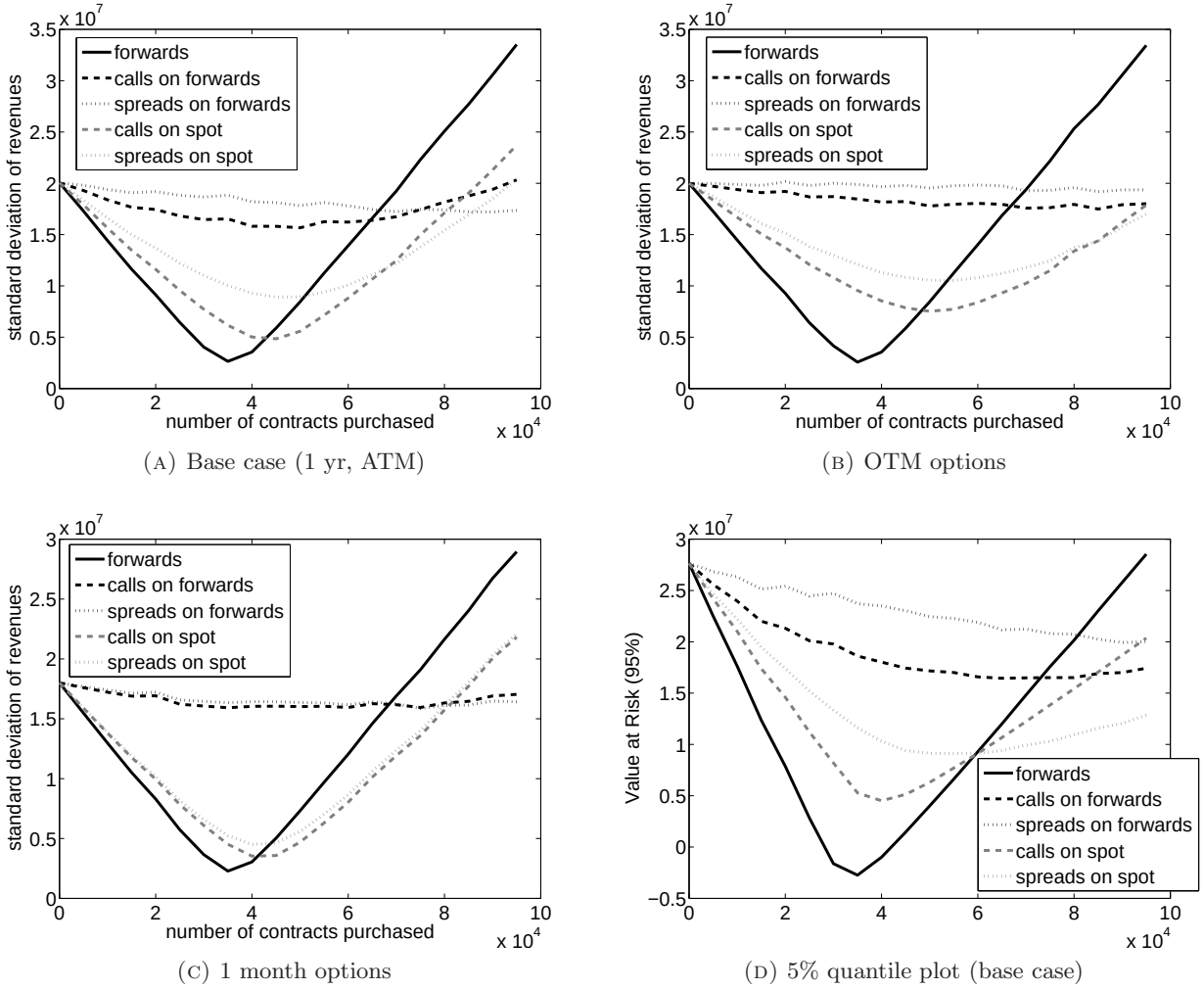

(A) Base case (1 yr, ATM)

(B) OTM options

(C) 1 month options

(D) 5% quantile plot (base case)

FIGURE 6. Comparison of variance reduction from different hedging strategies (forwards vs. various options) under several maturity and strike scenarios. Bottom right plot instead compares revenue quantile (95% value at risk).

In order to implement this hedging problem, we simulate 200,000 paths of load and price, calculating revenue for each path under different hedging strategies. In Figure 6, we can see the substantial benefit obtained from using derivative products to hedge risk. In all cases we can clearly observe an optimal hedge quantity on the plot, above which any further purchases increases the risk of the portfolio instead of hedging. However, there is significant variation in performance across products. When taken alone forward contracts are the most effective at variance reduction. This is perhaps not surprising since they shrink the entire distribution, instead of focusing on one tail of the distribution like options do. Nonetheless, due to the risk of power price spikes, the revenue distribution is significantly negatively skewed, and hence purchasing even out-of-the-money (OTM) call options can significantly reduce variance. (Though not plotted, the variance reduction

from buying puts is of course much less.)

The next most effective hedge after forward contracts is options on spot power, although it should be noted that these are rarely traded in practice. Spread options on spot power and gas provide slightly less variance reduction, since they essentially isolate and hedge only the risk of L_t and X_t, not the natural gas risk. Although such options are also rarely traded as financial contracts, the profits from a generating asset (ie, a power plant) are commonly approximated (by ignoring operational and transmission constraints) as spread options (for example, see [7]). Hence, buying a natural gas power plant can be quite an effective hedge for a power utility company in Texas, and moreover, in practice it is important to account for any generation assets when making hedging decisions. In addition, one should consider the purchases of natural gas required to operate the plant, which would offset the gas price exposure in power prices and potentially provide additional variance reduction. Finally we note that options on forwards provide substantially less variance reduction than options on spot since they do not provide protection against individual hourly spikes. In other words, deciding one day in advance on which hours to exercise your option is of course less effective than deciding after witnessing the spike!

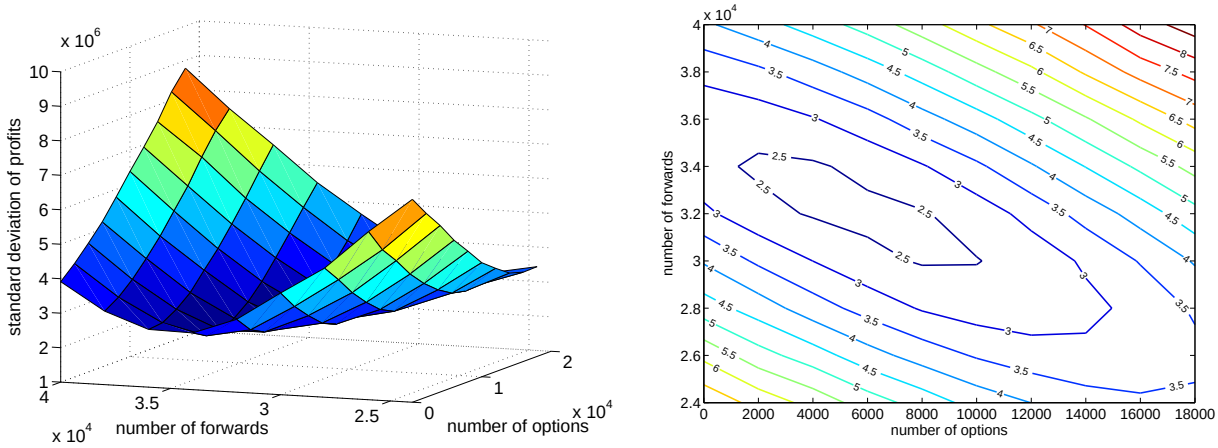

(A) Surface plot (B) Contour plot (all contour labels $\times 10^6$)

FIGURE 7. Variance reduction when trading in both options and forwards.

While the ranking of products by hedging effectiveness and the other features discussed above hold true throughout the four subplots of Figure 6, comparing the different scenarios in the subplots reveals other interesting insights. Whereas the base case plotted in Figure 6a corresponds to trading in ATM options, Figure 6b considers OTM options, with strikes 50% higher than in the ATM case. The effectiveness of variance reduction via options is somewhat reduced, since only a smaller portion of the tail of the distribution is affected. Since deep in-the-money call options behave much like forward contracts (except with an upfront premium), it is not surprising that higher strike calls move us further away from the hedging ability of forwards. Next, in Figure 6c, we shorten the maturity time T from one year to one month and observe a narrowing of the gap between call options and spread options in the plots. This is logical since the variance of gas price changes is much less over one month than over one year, while for load and other noise there is little change. Hence the one factor left unhedged by spread options is less significant one month before delivery. Finally, in the last plot (Figure 6d), we note that a utility company may instead be interested in risk measures other than variance, such as the quantile of the revenue distribution, or equivalently

the 'Value at Risk' of the loss distribution, a common risk management tool. Plotting the 95% Value at Risk (VaR), we observe that the relationship between the different hedging products is similar to the variance reduction case, with slight variations in the optimal purchase quantities.

In practice, energy companies typically own large portfolios of both physical and financial assets, which require continual monitoring and risk management. By combining several different products, such as forwards and options, even greater variance reduction may be possible than in our simple single product discussion above. We illustrate this in Figure 7, where purchases of both forwards and spot spread options are allowed. For clarity, we present the same results both as a surface plot and a contour plot. We can observe that a minimum in the variance surface appears somewhere in the middle, implying that simultaneously trading in the two products can provide further risk reduction than trading in either product alone. However, even in the static case, finding an optimal hedging portfolio across many maturities and many product types may require a sophisticated optimization algorithm, and hence we leave this for further work.

6. Conclusion

In this paper we have proposed and fitted a model for the Texas electricity market which is well suited to addressing common goals of energy companies, such as the pricing and hedging of portfolios of assets and load-serving obligations. As we have seen, the complexities of electricity markets require using models with numerous different components, designed to capture features ranging from high volatility and dramatic price spikes to subtle periodicities in load, price and their dependence structure. By proposing a structural model with two price regimes, we benefit from the clean price-to-load relationship of simple stack models, while still reproducing the noisy and characteristically spikey hourly price series often observed in historical data. Although electricity markets can vary widely from region to region and may require tailor-made models, we suggest that our framework is especially suited to spike-prone markets driven predominantly by a single fuel type, as is the case for ERCOT. Simulated spot prices from the model are found to match well with observed historical prices. Moreover, we obtain closed-form solutions for forward prices, which is of great benefit for both calibration and to reduce the computational burden which can sometimes accompany high-dimensional pricing and hedging applications. Closed-form prices for options are also available in several cases, including for spread options, products of particular importance in all energy markets. Lastly, through a simple revenue hedging example, we have illustrated one of the many practical uses of a joint price and load model for power, an important risk management tool for any firm exposed to the many intricacies and uncertainties of modern energy markets.

Appendix A. Pricing Result for Spread Options on Forwards

We begin by introducing convenient shorthand notation for the time-dependent functions given in (6)-(12). Since we are now pricing an option on a forward, there are three relevant time points ($t < T < T_f$), and we need notation for the three possible variations of these expressions, for example $\sigma_L(t,T)$, $\sigma_L(T,T_f)$ and $\sigma_L(t,T_f)$. As before, we use simply σ_L for the first case, but now introduce $\tilde{\sigma}_L$ and $\hat{\sigma}_L$ for the second and third cases:

$$\sigma_L = \sigma_L(t,T), \quad \tilde{\sigma}_L = \sigma_L(T,T_f), \quad \hat{\sigma}_L = \sigma_L(t,T_f).$$

We apply the same convention to $\sigma_X, \mu_L, \mu_X, \rho, k_i, l_i$, letting 'tilde' mean (T,T_f) and 'hat' mean (t,T_f). We now price at time t a spark spread option (with given heat rate h, and maturity T) on power and gas forwards (with maturities T_f) as follows:

$$\begin{aligned}
\tilde{V}_t^{p,g} &= \mathrm{e}^{-r(T-t)}\mathbb{E}_t^{\mathbb{Q}}\left[\mathbb{E}_t^{\mathbb{Q}}\left[\left(F^p(T,T_f) - hF^g(T,T_f)\right)^+ | L_T\right]\right] \\
&= \mathrm{e}^{-r(T-t)}F^g(t,T_f)\mathbb{E}_t^{\mathbb{Q}}\left[\left(\exp\left(\tilde{k}_1 + \tilde{l}_1\tilde{\mu}_L + \frac{1}{2}\tilde{l}_1^2\tilde{\sigma}_L^2\right)\left(1 - p_s\Phi\left(\frac{\tilde{\mu}_L - \mu_s + \tilde{l}_1\tilde{\sigma}_L^2}{\sqrt{\tilde{\sigma}_L^2 + \sigma_s^2}}\right)\right)\right.\right. \\
&\qquad \left.\left. + \exp\left(\tilde{k}_2 + \tilde{l}_2\tilde{\mu}_L + \frac{1}{2}\tilde{l}_2^2\tilde{\sigma}_L^2\right) p_s\Phi\left(\frac{\tilde{\mu}_L - \mu_s + \tilde{l}_2\tilde{\sigma}_L^2}{\sqrt{\tilde{\sigma}_L^2 + \sigma_s^2}}\right) - h\right)^+\right]
\end{aligned}$$

We now reiterate our assumption that $F^p(T,T_f)$ (and hence the expression in the expectation above) can be approximated to be independent of X_T, given the very rapid mean reversion speed of X. This simplifies the calculation to a one-dimensional integral, which is solved via the more general version of (13) for definite integrals. Eventually, we get

$$\begin{aligned}
\tilde{V}_t^{p,g} &= \mathrm{e}^{-r(T-t)}F^g(t,T_f)\left\{\mathrm{e}^{A_1}\Phi\left(-\frac{L^\star - \mu_L - \beta_1\sigma_L^2\mathrm{e}^{-\kappa_L(T_f-T)}}{\sigma_L}\right) - h\Phi\left(-\frac{L^\star - \mu_L}{\sigma_L}\right)\right. \\
&\qquad \left. + p_s\sum_{i=1}^{2}(-1)^i\mathrm{e}^{A_i}\varphi\left(\frac{L^\star - \mu_L - \beta_i\sigma_L^2\mathrm{e}^{-\kappa_L(T_f-T)}}{\sigma_L}, \frac{\hat{\mu}_L - \mu_s + \hat{l}_i\hat{\sigma}_L^2}{\sqrt{\hat{\sigma}_L^2 + \sigma_s^2}}; \frac{-\sigma_L\mathrm{e}^{-\kappa_L(T_f-T)}}{\sqrt{\hat{\sigma}_L^2 + \sigma_s^2}}\right)\right\} \qquad (18)
\end{aligned}$$

where

$$\varphi(x,y;\lambda) = \Phi(y) - \Phi_2(x,y;\lambda)$$

and for $i \in \{1,2\}$,

$$A_i = \hat{k}_i + \hat{l}_i\hat{\mu}_L + \frac{1}{2}\hat{l}_i^2\hat{\sigma}_L^2.$$

Finally $L^\star$ is defined to be the value of load at time T above which the option is in-the-money and thus satisfies $F^p(T,T_f) = hF^g(T,T_f)$, or equivalently $L^\star = \bar{L}_T$ such that

$$\begin{aligned}
&\exp\left(\tilde{k}_1 + \tilde{l}_1\tilde{\mu}_L + \frac{1}{2}\tilde{l}_1^2\tilde{\sigma}_L^2\right)\left(1 - p_s\Phi\left(\frac{\tilde{\mu}_L - \mu_s + \tilde{l}_1\tilde{\sigma}_L^2}{\sqrt{\tilde{\sigma}_L^2 + \sigma_s^2}}\right)\right) \\
&\qquad + \exp\left(\tilde{k}_2 + \tilde{l}_2\tilde{\mu}_L + \frac{1}{2}\tilde{l}_2^2\tilde{\sigma}_L^2\right) p_s\Phi\left(\frac{\tilde{\mu}_L - \mu_s + \tilde{l}_2\tilde{\sigma}_L^2}{\sqrt{\tilde{\sigma}_L^2 + \sigma_s^2}}\right) = h.
\end{aligned}$$

where the dependence on $\bar{L}_T$ appears in $\tilde{\mu}_L$ and hence also in $\tilde{k}_1$ and $\tilde{k}_2$. In our experience with the ERCOT market parameters, we find that a unique $L^\star$ always exists for any $h > 0$. We also note that as $h \to 0$, $L^\star \to -\infty$, and (18) converges to $\mathrm{e}^{-r(T-t)}F^p(t,T_f)$, which is given by (14).

Acknowledgements

The research was supported by the SAP Initiative for Energy Systems Research, as well as the National Science Foundation. In particular, the first author had partial support from NSF grant DMS-0739195, the second author from NSF grant CMMI-0856153, and the third author from NSF grant DMS-0807440. The authors would also like to offer special thanks to Tong Song at NRG for posing the problem and his guidance of the research.

References

[1] R. Aïd, L. Campi, Adrien N. Huu, and N. Touzi. A structural risk-neutral model of electricity prices. *International Journal of Theoretical and Applied Finance*, 12:925–947, 2009.

[2] R. Aïd, L. Campi, and N. Langrené. A structural risk-neutral model for pricing and hedging power derivatives. *Mathematical Finance*. Published online Feb. 13, 2012.

[3] M. Barlow. A diffusion model for electricity prices. *Mathematical Finance*, 12(4):287–298, 2002.

[4] F.E. Benth, J.S. Benth, and S. Koekebakker. *Stochastic Modeling of Electricity and Related Markets*. World Scientific.

[5] M. Burger, B. Klar, A. Müller, and G. Schindlmayr. A spot market model for pricing derivatives in electricity markets. *Quantitative Finance*, 4:109–122, 2004.

[6] R. Carmona and M. Coulon. A survey of commodity markets and structural models for electricity prices. In F. E. Benth, V. Kholodnyi, and P. Laurence, editors, *Quantitative Energy Finance: Modeling, Pricing and Hedging in Energy and Commodity Markets*. 2013.

[7] R. Carmona, M. Coulon, and D. Schwarz. Electricity price modeling and asset valuation: a multi-fuel structural approach. *Mathematics and Financial Economics*, 7(2):167–202.

[8] A. Cartea and M. Figueroa. Pricing in electricity markets: A mean reverting jump diffusion model with seasonality. *Applied Mathematical Finance*, 12(4):313–335, 2005.

[9] A. Cartea, M. Figueroa, and H. Geman. Modelling electricity prices with forward-looking capacity constraints. *Applied Mathematical Finance*, 16(2):103–122, 2009.

[10] A. Cartea and P. Villaplana. Spot price modeling and the valuation of electricity forward contracts: the role of demand and capacity. *Journal of Banking and Finance*, 32:2501–2519, 2008.

[11] M. Coulon and S. Howison. Stochastic behaviour of the electricity bid stack: from fundamental drivers to power prices. *Journal of Energy Markets*, 2:29–69, 2009.

[12] C. De Jong and R. Huisman. Option pricing for power prices with spikes. *Energy Power Risk Management*, 7:12–16, 2003.

[13] A. Eydeland and H. Geman. Pricing power derivatives. *Risk Magazine*, 10:71–73, 1998.

[14] H. Geman and A. Roncoroni. Understanding the fine structure of electricity prices. *Journal of Business*, 79, 2006.

[15] Robert Geske. The valuation of compound options. *Journal of Financial Economics*, 7:63–81, 1979.

[16] B. Hambly, S. Howison, and T. Kluge. Modelling spikes and pricing swing options in electricity markets. Technical report, 2009.

[17] J. Hull and A. White. Pricing interest-rate derivative securities. *The Review of Financial Studies*, 3(4):573–592, 1990.

[18] J.H. Kim and W.B. Powell. An hour-ahead prediction model for heavy-tailed spot prices. *Energy Economics*, 33:1252–1266, 2011.

[19] M. Lyle and R. Elliott. A "simple" hybrid model for power derivatives. *Energy Economics*, 31:757–767, 2009.

[20] C. Pirrong and M. Jermakyan. The price of power: The valuation of power and weather derivatives. *Journal of Banking and Finance*, 32:2520–2529, 2008.

[21] E. Schwartz. The stochastic behaviour of commodity prices: Implications for valuation and hedging. *The Journal of Finance*, 3:923–973, 1997.

[22] P. Skantze, A. Gubina, and M. Ilic. Bid-based stochastic model for electricity prices: the impact of fundamental drivers on market dynamics. MIT E-lab report, November 2000.

[23] A.E.D. Veraart and L.A.M. Veraart. Modelling electricity day-ahead prices by multivariate lvy semistationary processes. In F. E. Benth, editor, *Financial Engineering for Energy Asset Management and Hedging in Commodity Markets; Proceedings from the special thematic year at the Wolfgang Pauli Institute, Vienna*. 2012.

[24] R. Weron, M. Bierbrauer, and S. Truck. Modeling electricity prices: jump diffusion and regime switching. *Physica A: Statistical Methods and its Applications*, 336:39–48, 2004.